

# **Tension Testing of 8-in. (200-mm) Diameter TR-XTREME™ Ductile Iron pipe with HDSS Quiklok**

**Shih-Hung Chiu**

**Shakhzod Takhirov**

**Kenichi Soga**



**Berkeley**  
**CENTER FOR**  
**Smart Infrastructure**

CSI Report 2024/04  
Center for Smart Infrastructure (CSI)  
Department of Civil and Environmental Engineering  
University of California, Berkeley September 2024

## EXECUTIVE SUMMARY

This report presents the experimental results of a tension test conducted on an 8-inch TR-XTREME™ earthquake-resistant ductile iron pipe, equipped with the HDSS Quiklok on spigot as locking mechanism, manufactured by U.S. Pipe. The primary objective of the test was to evaluate the ultimate performance of the jointed pipeline system using the HDSS Quiklok in comparison to a factory-manufactured weld bead on the spigot. The results show that the ultimate axial pulling capacity of the specimen with HDSS Quiklok is comparable to that of the weld bead although the failure pattern varies. In addition, distributed fiber optic strain sensors were installed to capture the strain development profile in both the longitudinal and circumferential directions. This data provides insights into the joint failure mechanism, offering a deeper understanding of the structural behavior under tensile loading condition.

**Keywords:** *Ductile iron pipe, jointed water pipelines, fiber optic sensing.*

## **ACKNOWLEDGMENTS**

The East Bay Municipal Utility District (EBMUD) requested this test, and U.S. Pipe provided the funding and supplied the pipes used for the experiment. Completing the work would not be possible without the support of John Kochan, Irik Larson, and Phillip Wong of the University of California, Berkeley. Active involvement and guidance from Jeff Mason of U.S. Pipe, Pongsiri (Eng) Prachyaratanawooti and David Katzev and of EBMUD are greatly appreciated.

## **DISCLAIMER**

Any opinions, findings, conclusions, or recommendations expressed in this report are those of the author(s) and do not necessarily reflect those of the University of California, Berkeley.

# CONTENTS

EXECUTIVE SUMMARY .....	II
ACKNOWLEDGMENTS .....	III
DISCLAIMER.....	IV
CONTENTS .....	V
LIST OF FIGURES.....	VI
LIST OF TABLES.....	VII
<b>1. Introduction .....</b>	<b>8</b>
<b>2. Test Setup .....</b>	<b>10</b>
<b>3. Instrumentation .....</b>	<b>11</b>
3.1 Conventional Instruments.....	11
3.2 Distributed Fiber Optic Sensors.....	12
<b>4. Test Results.....</b>	<b>13</b>
4.1 Failure Mode.....	15
4.2 Axial Strains.....	16
4.3 Hoop Strains.....	19
<b>5. Conclusion.....</b>	<b>23</b>
<b>6. Reference.....</b>	<b>25</b>
<b>Appendix A: Distributed Fiber Optic Sensing .....</b>	<b>26</b>

## LIST OF FIGURES

Figure 1-1 Mechanism of TR-XTREMETM joint (U.S. Pipe, 2024).....	8
Figure 1-2 Recommended installation positions (U.S. Pipe, 2024).....	9
Figure 1-3 HDSS QuikLok .....	9
Figure 2-1 Experimental setup design .....	10
Figure 2-2 Overview of the experimental setup .....	10
Figure 3-1 Instrumentation plan of position transducers .....	11
Figure 3-2 Installation of position transducer.....	12
Figure 3-3 DFOS instrumentation plan.....	13
Figure 4-1 Axial force, average joint opening, and water pressure results.....	14
Figure 4-2 Failure of the Specimen. (a) tensile failure at the circumference of the groove, (b) failed off snap ring .....	15
Figure 4-3 Sketch of Specimen-HDSS failure mode.....	16
Figure 4-4 Failure of previous tests that the specimens were equipped with factory-manufactured weld bead on the spigot (Chiu et al., 2023) (a) Weld bead failure on spigot of Specimen-WB1 (b) Bell failure of Specimen-WB2.....	16
Figure 4-5 Axial strain vs. load.....	17
Figure 4-6 Axial strain development of bell pipe under 180-kips loading condition. (a) North side, (b) Top side, (c) Bottom side, (d) South side .....	18
Figure 4-7 Bell deformation mechanism .....	18
Figure 4-8 Axial strain development of spigot under 180-kips loading condition. (a) North side, (b) Top side, (c) Bottom side, (d) South side.....	19
Figure 4-9 Strain distribution in the circumferential direction under 180-kips loading condition. ....	21
Figure 4-10 Waterfall plot of sensors on the bell and spigot (a) Sensor 6 (b) Sensor 7 .....	22
Figure 4-11 Sketch of squatting mechanism (a) Specimen-HDSS (b) Specimen-WB1 & Specimen-WB2 .....	23

## LIST OF TABLES

Table 3-1 Conventional instrumentation local names .....	11
Table 3-2 Schematic illustration of the selected strain sensor cable (Wu et al., 2015) .....	12
Table 3-3 DFOS local names.....	13
Table 4-1 Comparison of the results of the ERDIP tension tests (Note that the “Water Leakage Joint Opening” is measured from the fully extracted location) .....	14

# 1. Introduction

This report presents the experimental results of a tension test conducted on an 8-inch TR-XTREME™ earthquake-resistant ductile iron pipe specimen, manufactured by U.S. Pipe. The pipe is designed to maintain full water service during seismic events to enhance the seismic resiliency of pipeline systems. It features a single-restrained bell joint, allowing 2.9 inches of horizontal movement and a 5-degree allowable deflection capacity, with a schematic of the bell joint shown in Figure 1-1.

In standard installations, the spigot is inserted into the bell through a water-prevent rubber gasket, typically equipped with a weld bead to bear against the locking segments as a locking mechanism during axial pulling. The bell joint features a single slot for inserting the locking segments that are contained within a cavity in the bell, and three white stripes on the spigot guide the correct installation position, as shown in Figure 1-2. The manufacturer recommends three positions: collapsed, midpoint, and extended. In this test, the spigot started in the fully extended position (Option C), with the snap ring already in contact with the locking segments.

However, on-site pipe cutting can remove the factory-installed weld bead. To address this, U.S. Pipe offers the HDSS QuikLok system, which allows installers to cut, groove, and install a snap ring onto the spigot, preserving the strength and deflection capacity of the original joint while providing field flexibility. For this experiment, the HDSS QuikLok was installed in place of the weld bead, as illustrated in Figure 1-3.

In this study, a horizontal force was applied to the spigot, forcing it to move out of the joint. The objectives of the test were: (1) to characterize the joint with HDSS QuikLok's response to axial force beyond its horizontal movement limit and (2) to compare the performance of the HDSS QuikLok system to the factory-installed weld bead on spigot. Distributed fiber optic sensors (DFOS) were used to continuously measure strain development in both the longitudinal and circumferential directions of the pipeline.

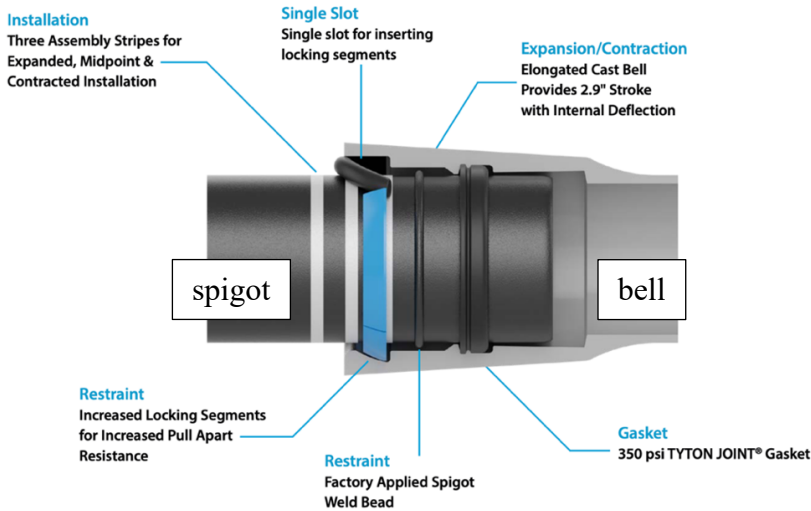
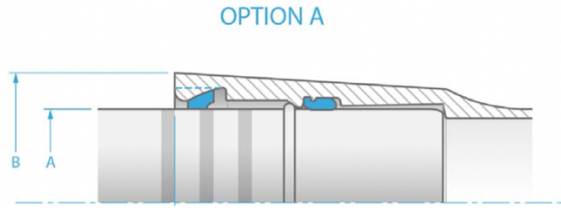
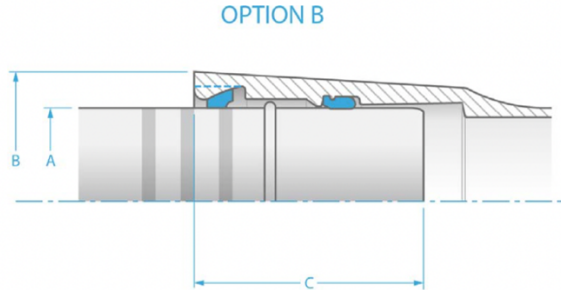


Figure 1-1 Mechanism of TR-XTREME™ joint (U.S. Pipe, 2024)

**Option A-Collapsed** – Correct assembly is determined when the front edge of the assembly stripe furthest from the spigot tip lines up with the face of the pipe bell as viewed from above, leaving only one assembly stripe shown.



**Option B-Midpoint** – Correct assembly is determined when the front edge of the middle assembly stripe lines up with the face of the pipe bell as viewed from above, leaving two assembly stripes shown.



**Option C-Extended (Restrained)** - Correct assembly is determined when the front edge of the assembly stripe closest to the spigot tip lines up with the face of the pipe bell as viewed from above, leaving three assembly stripes shown. This is the proper assembly when immediate joint restraint is required.

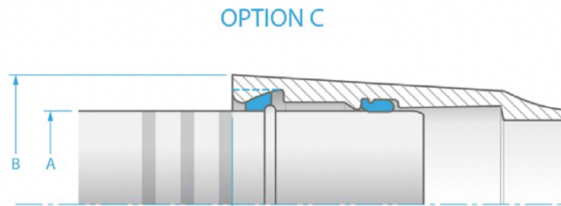


**Figure 1-2 Recommended installation positions (U.S. Pipe, 2024)**



**Figure 1-3 HDSS QuikLok**

# 2. Test Setup

The experimental setup for this study was developed at the Center for Smart Infrastructure (CSI) at UC Berkeley. The design of the experimental setup is shown in Figure 2-1. A self-reacting frame was designed to accommodate both the loading and reaction sections. The system employed a hydraulic actuator with a compression capacity of 314 kips and a total stroke of 12 inches. To restrain the pipeline, two specially designed jackets were utilized. The hydraulic actuator applied force to the spigot through a loading fixture, which bore against the weld bead at the pipe's end. A similar mechanism was used to secure the bell pipe to the reaction beam. An overview of the experimental setup is shown in Figure 2-2.

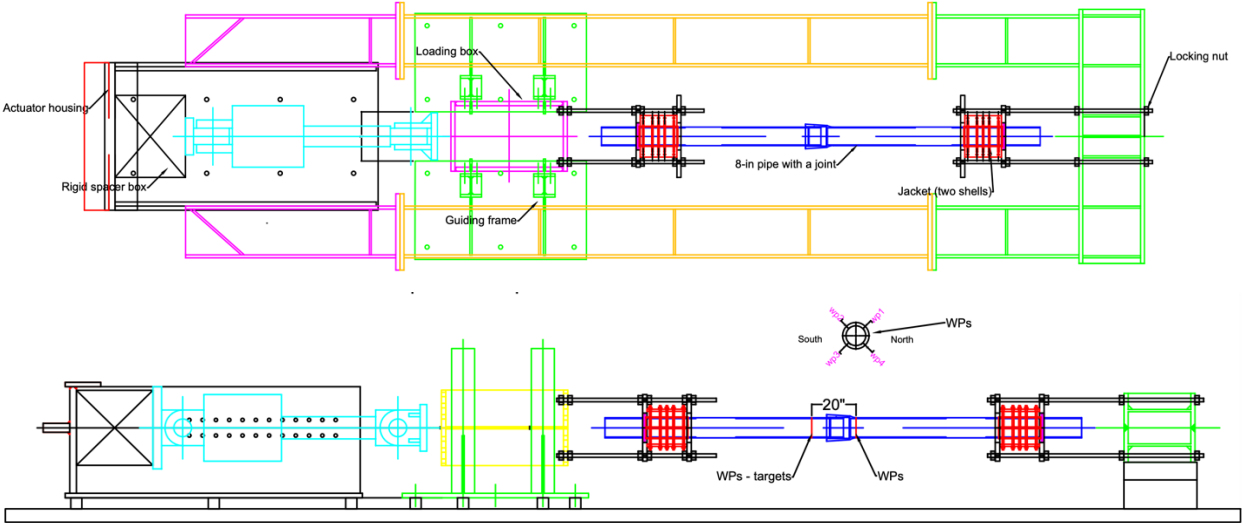


Figure 2-1 Experimental setup design



Figure 2-2 Overview of the experimental setup

The 8-inch diameter TR-XTREME™ pipes, made of ductile iron and manufactured by U.S. Pipe, were tested in their extended position, where the locking segments were in contact with the snap ring on the spigot at the initial stage. During the experiment, the pipes were pressurized to approximately 70 psi. The hydraulic actuator then applied axial force to pull the spigot until significant failure occurred, followed by severe water leakage.

### 3. Instrumentation

The instrumentation consisted of conventional instruments (wire pots, load cell) and distributed fiber optic sensors (DFOS).

#### 3.1 Conventional Instruments

The locations of the instruments are shown in Figure 3-1, and the local instrumentation names are shown in Table 3-1. Four position transducers (or wired pots herein) were placed on the bell pipe at 45 degrees apart from the quarter points around the circumference and were fixed to the spigot to measure the joint opening. The installation of the wired pots is shown in Figure 3-2.

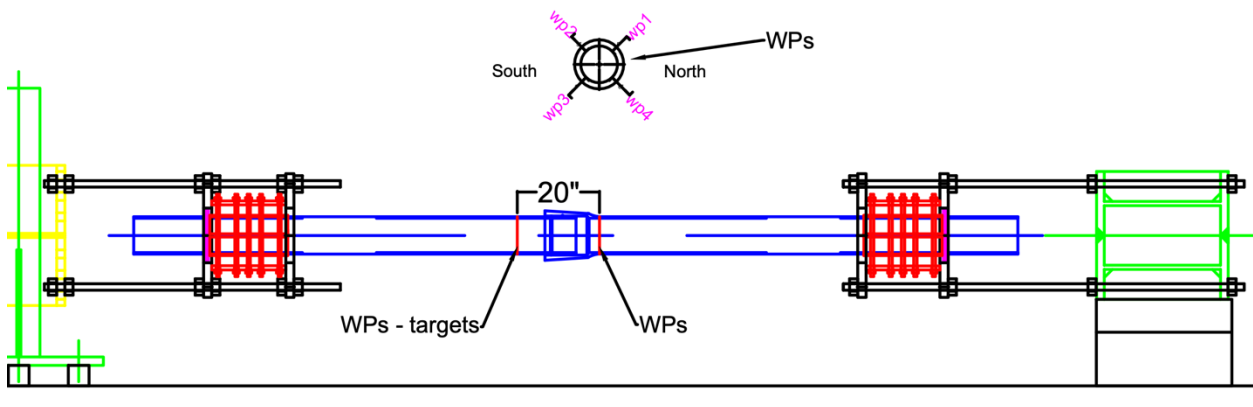


Figure 3-1 Instrumentation plan of position transducers

Table 3-1 Conventional instrumentation local names

Instrument	Location	Local Instrument Name
Wired Pot	Parallel to Axial Direction, East of Bell, Top-north	wp1
	Parallel to Axial Direction, East of Bell, Top-south	wp2
	Parallel to Axial Direction, East of Bell, Bottom-south	wp3
	Parallel to Axial Direction, East of Bell, Bottom-north	wp4

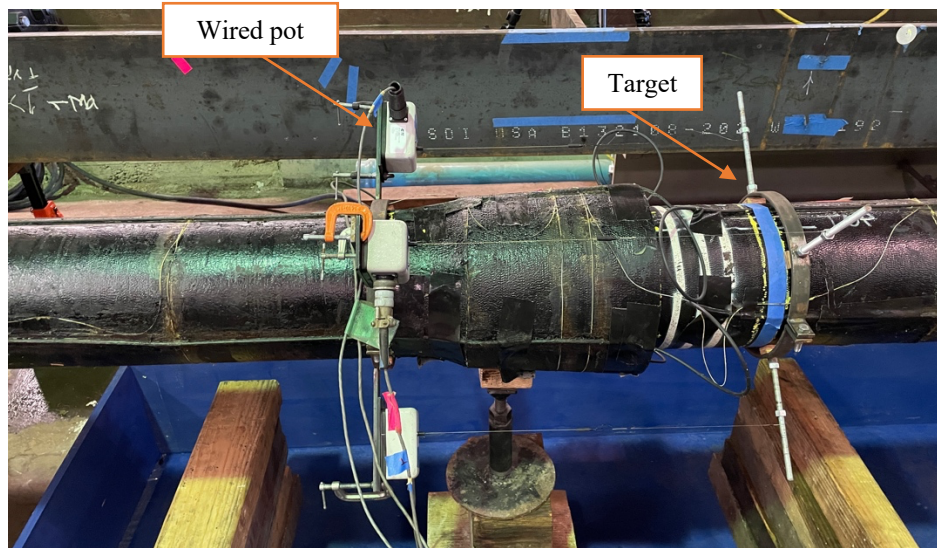
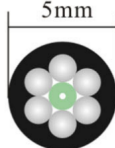
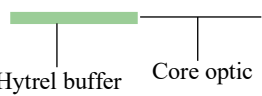
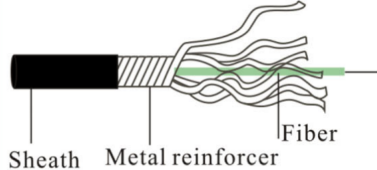


Figure 3-2 Installation of position transducer

### 3.2 Distributed Fiber Optic Sensors

Two types of fiber optic cables manufactured by NanZee Sensing Technology Co. were used as shown in Table 3-2; (a) 5 mm diameter armored cable (NanZee 5mm) and (b) 0.9 mm diameter cable (NanZee 0.9mm). The local instrument names are listed in Table 3-3, and the layouts of the cables are shown in Figure 3-3. Huntsman Araldite 2021-1 epoxy was used to attach the cables to the pipes.

Table 3-2 Schematic illustration of the selected strain sensor cable (Wu et al., 2015)

Brand	NanZee Sensing Technology Co.	NanZee Sensing Technology Co.
Model	NZS-DSS-C07	NZS-DSS-C02
Cross section		
Side view		

NanZee 5mm cables (blue lines), which are commonly used in the field due to their robustness, were used in the longitudinal direction to check their performance for actual field application. They were attached on both pipes, 90 degrees apart, numbered F10-F17. To better understand the deformation mechanism of the pipes and bell section, NanZee 0.9mm cables (red lines), which are fragile but cost-effective in laboratory conditions, were used for measuring circumferential strains, numbered F1-F9. Four circumferential sensors with about 16-inch spacing were installed on both pipes. In addition, another three circumferential sensors were

attached to the bell end, the middle of the section, and the location on top of the locking segments (i.e., about 3.5 inches from the bell face).

A Rayleigh-based optical frequency domain reflectometry (OFDR), Luna ODiSI 6100 series (LUNA, 2022), was used in this experiment for data acquisition. The analyzer is capable of measuring up to 100 meters long fiber optic cable with an accuracy of less than  $\pm 1$  micro strain when taking a measurement every 0.65mm. Further details about the cables and analyzer can be found in Appendix A.

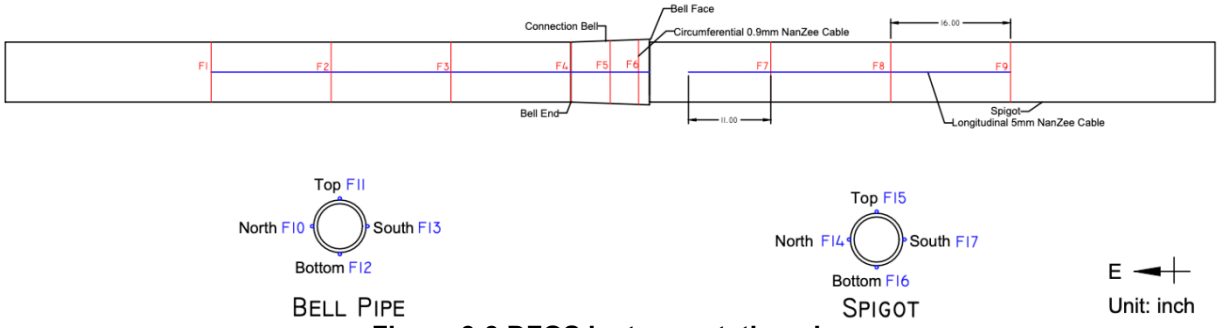


**Figure 3-3 DFOS instrumentation plan**

**Table 3-3 DFOS local names**

Instrument	Location	Local Instrument Name
DFOS	58.5 inches east of bell face, Circumferential	F1
	42.5 inches east of bell face, Circumferential	F2
	26.5 inches east of bell face, Circumferential	F3
	Bell end, Circumferential	F4
	Mid location of bell, Circumferential	F5
	3.5 inches east of bell face Circumferential	F6
	16 inches south of bell face, Circumferential	F7
	32 inches south of bell face, Circumferential	F8
	48 inches south of bell face, Circumferential	F9
	Bell pipe, North, Longitudinal	F10
	Bell pipe, Top, Longitudinal	F11
	Bell pipe, Bottom, Longitudinal	F12
	Bell pipe, South, Longitudinal	F13
	Spigot, North, Longitudinal	F14
	Spigot, Top, Longitudinal	F15
	Spigot, Bottom, Longitudinal	F16
	Spigot, South, Longitudinal	F17

## 4. Test Results

All test results are discussed in this section. In addition, a summary of the failure mode and performance of the 8 inches TR-XTREME™ ductile iron pipe equipped with HDSS QuikLok on spigot is included.

In this experiment, the pipes were filled with water and pressurized to 70 psi. A monotonic force was applied along the spigot's longitudinal axis, and four wire pots, positioned 90 degrees apart around the circumference of the bell pipe, were used to measure joint opening. The average joint opening, calculated from the wire pot readings, and the axial force results are shown in Figure 4-1. The maximum axial force reached 190.3 kips, with an average joint opening of 0.5 inches. Water pressure drops were observed at the point of maximum axial force.

The ultimate axial force performance of the present test was similar to those of the specimens with factory-manufactured weld bead that were previously tested at the Center for Smart Infrastructure (Chiu et al., 2023). However, the failure location and water leakage time varied.

Table 4-1 summarizes the performance of the three tension tests conducted. Specimen-WB1 and Specimen-WB2 refer to the previous tests that the specimens were equipped with factory-manufactured weld bead on the spigot. The difference between these two specimens are the end weld bead which are used for transfer the force from the actuator to the specimen. In Specimen-WB1, the end weld bead failed before a significant pipe failure. Therefore, Specimen-WB2 was equipped with double-sided weld (trust collar), which provided a much stronger end weld bead. As a consequence, the bell failed when the applied force reached 174-kips. No water leakage was found at this stage. The pipe was still capable of maintaing water service not until an additional 2.9 inches of axial movement.

In contrast, Specimen-HDSS (tested with HDSS QuikLok) exhibited slightly higher ultimate axial resistance, but water leakage occurred immediately after the peak load failure. This variation in performance is attributed to different failure mechanisms, which will be discussed in the next section.

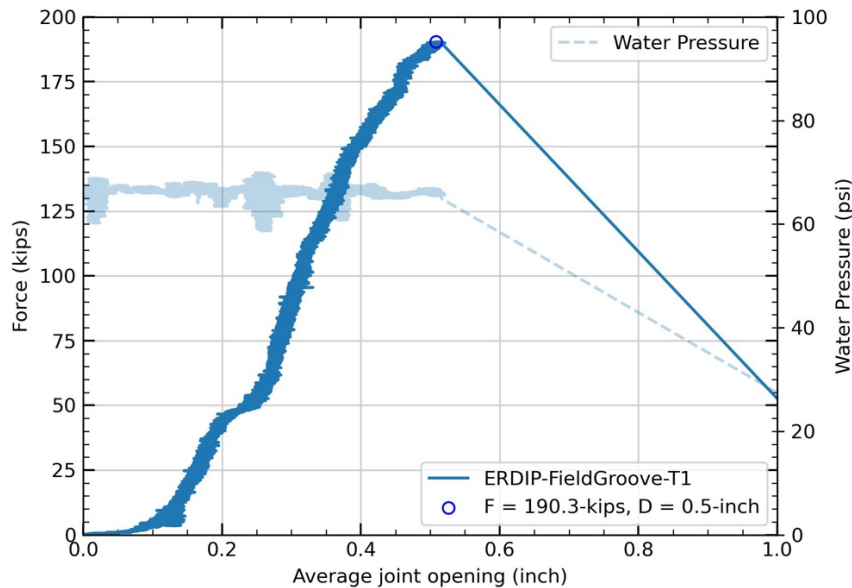


Figure 4-1 Axial force, average joint opening, and water pressure results

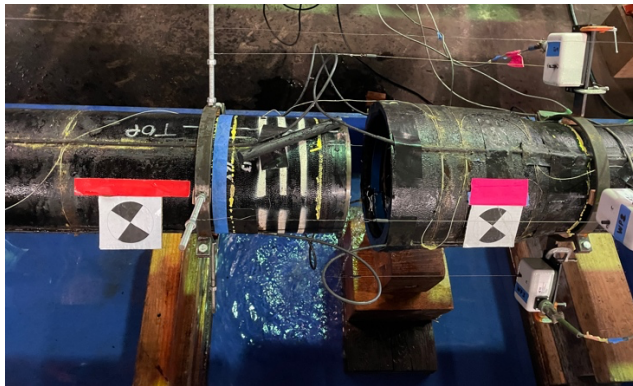
Table 4-1 Comparison of the results of the ERDIP tension tests (Note that the “Water Leakage

Joint Opening” is measured from the fully extracted location)

	Specimen-WB1	Specimen-WB2	Specimen-HDSS
<b>Locking Mechanism</b>	Weld bead	Weld bead	HDSS QuikLok
<b>Max. Load (kips)</b>	188	174	190
<b>Water Leakage Joint Opening (in.)</b>	N/A	2.9	0.5
<b>Failed Section</b>	Weld bead on spigot	Bell	Spigot
<b>Test Date</b>	4/27/22	7/15/22	7/11/24
<b>End weld bead</b>	Single weld	Double-sided weld (trust collar)	Double-sided weld (trust collar)

#### 4.1 Failure Mode

The test concluded at a force of 190.3 kips when the spigot failed and the pipe experienced severe water leakage at the same time. As shown in Figure 4-2 (a), the spigot experienced a tensile failure at its groove. The thinner wall and the snap ring's pressure against the locking segment likely caused high stress concentration. This resulted in a full circumferential tensile failure around the groove, leaving a portion of the pipe trapped in the bell. The snap ring fell off as the groove failed, as shown in Figure 4-2 (b). Water leaked immediately when the spigot failed. The spigot was pulled out, as shown in Figure 4-3, rendering it incapable of holding water.



(a)



(b)

**Figure 4-2 Failure of the Specimen. (a) tensile failure at the circumference of the groove, (b) failed off snap ring**

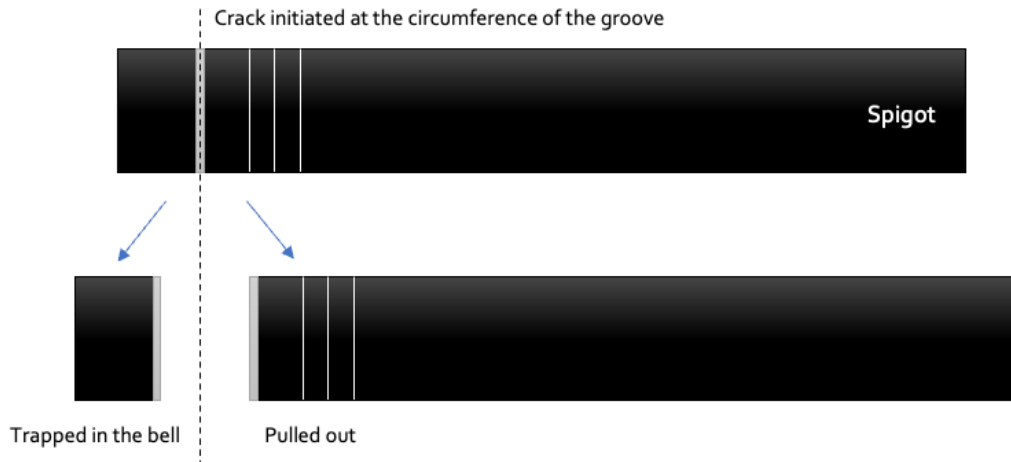


**Figure 4-3 Sketch of Specimen-HDSS failure mode**

In the previous tension tests ([Chiu et al., 2023](#)), water remained contained despite a crack in the bell (see Figure 4-4(b)). Even with a crack on the bell, the rubber gasket inside the bell sealed the water until further axial movement caused leakage. In summary, while the ultimate axial force capacity between the specimen with a weld bead and the one with HDSS QuikLok were similar, the failure mechanisms differed, resulting in different timing for water leakage.

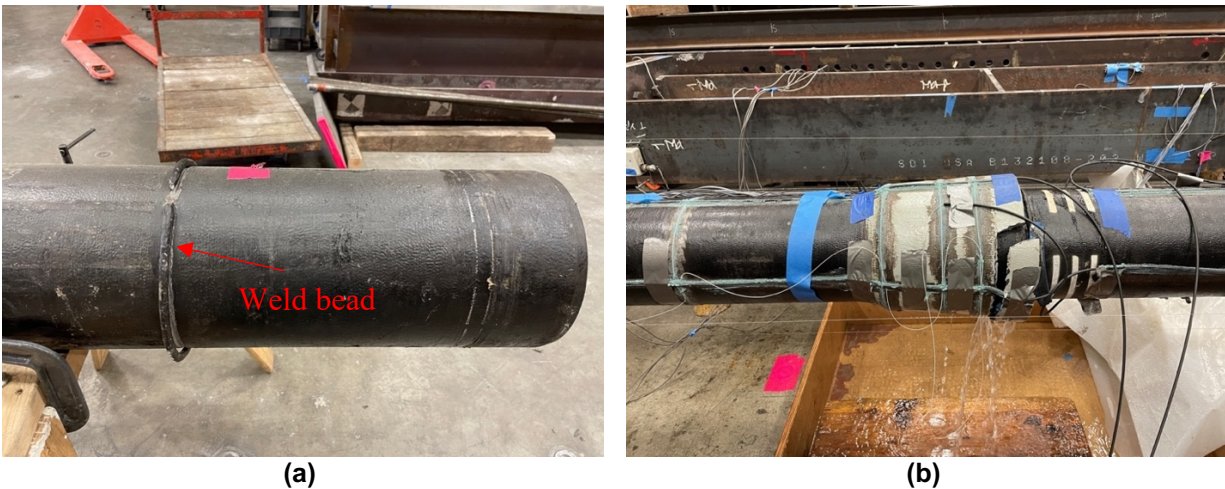


**Figure 4-4 Failure of previous tests that the specimens were equipped with factory-manufactured weld bead on the spigot (Chiu et al., 2023) (a) Weld bead failure on spigot of Specimen-WB1 (b) Bell failure of Specimen-WB2**

## 4.2 Axial Strains

The axial strain data collected from the DFOS sensors are presented in Figure 4-5, illustrating the relationship between axial strain and axial load. Measurements were taken at the midpoints of F2 and F3 (bell pipe) and F7 and F8 (spigot) using longitudinal sensors. As the monotonic force was applied along the longitudinal axis of the pipe, the resulting axial strains were all tensile. The strain magnitudes for both the bell pipe and the spigot are comparable,

suggesting an effective transfer of force through the locking mechanism (i.e., snap ring and locking segments).

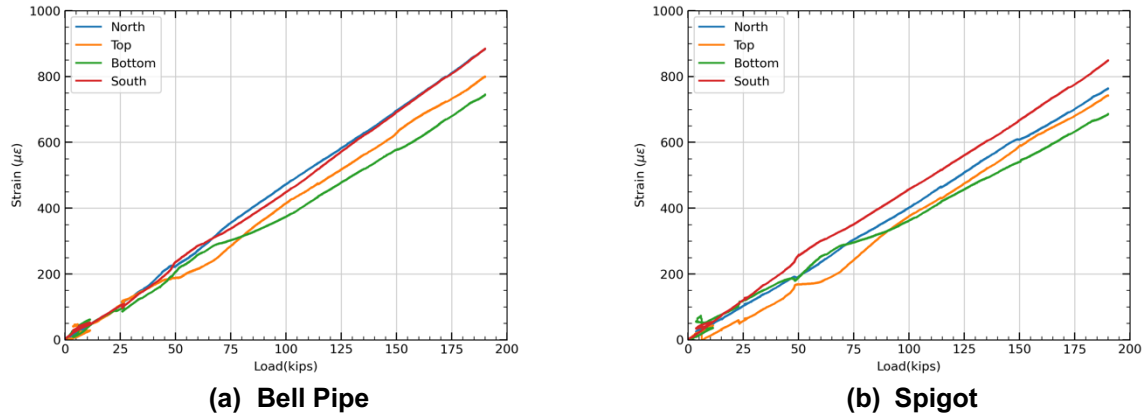
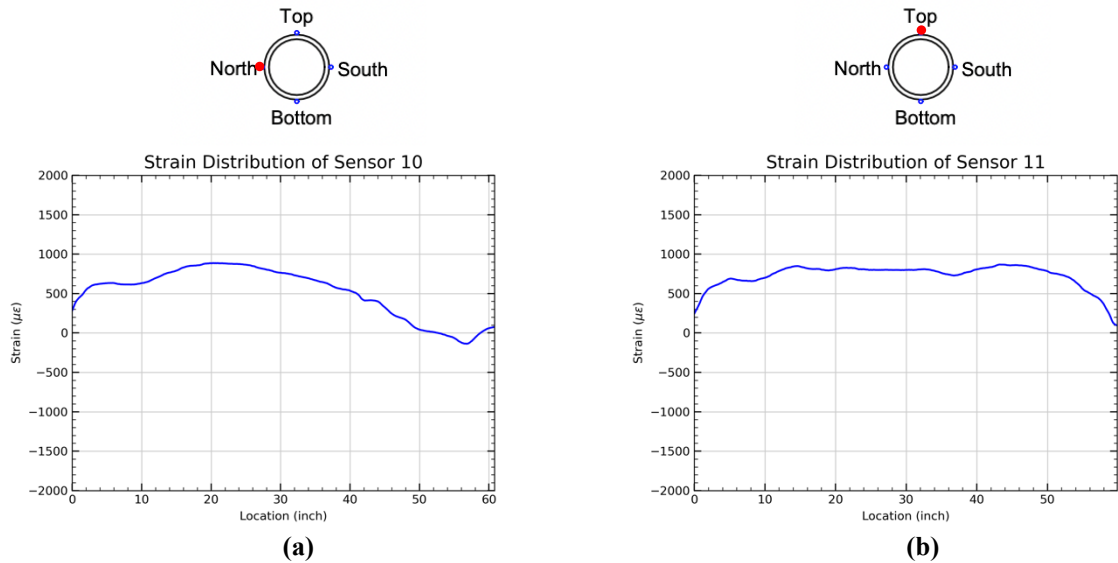
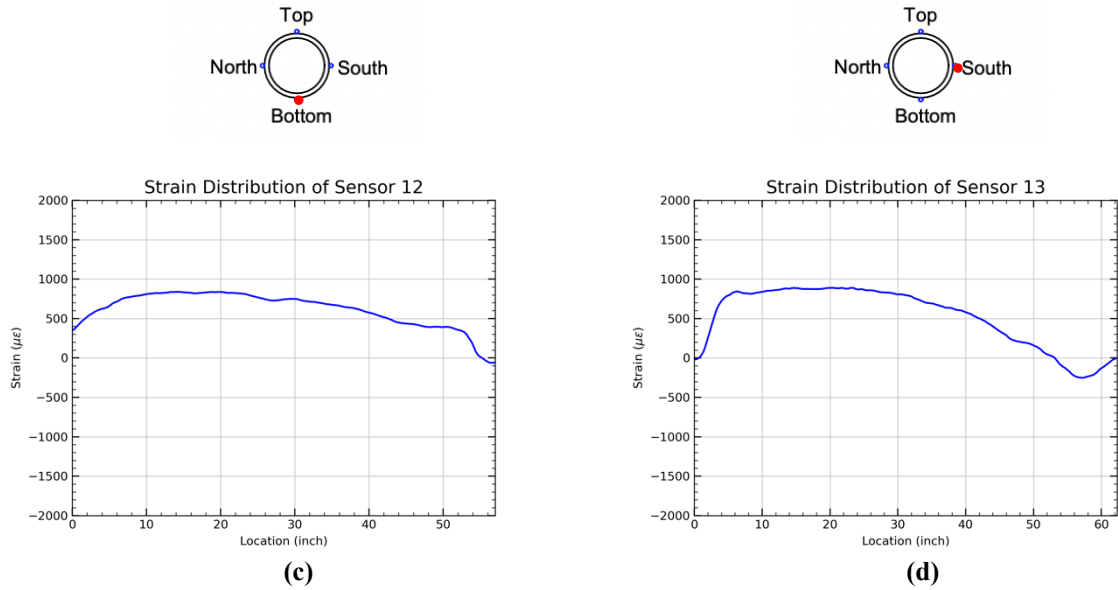


Figure 4-5 Axial strain vs. load

Figure 4-6 illustrates the axial strain distribution under a 180-kip force as measured on the bell pipe. While the majority of the pipe experienced tensile strains due to the applied tensile force, compressive strains were observed on the north, south, and bottom sides of the bell (around the 50-60 inch mark). This phenomenon likely occurred as the spigot was being pulled out, causing the snap ring to bear against the locking segments. As the locking segments pushed outward, the bell bent locally at the locking segment location. This resulted in compressive stress developing on its outer surface, as depicted in Figure 4-7.

This localized bending behavior was less pronounced on the top side of the bell for two reasons. First, no locking segments were placed on the top side; instead, a rubber retainer was used to position the other locking segments. Since the rubber gasket has lower stiffness and is compressible, it did not cause the bell to bend much at this location. Second, there is a gap on the top side of the snap ring for installation purposes, preventing direct force transfer at that specific location.





**Figure 4-6 Axial strain development of bell pipe under 180-kips loading condition. (a) North side, (b) Top side, (c) Bottom side, (d) South side**

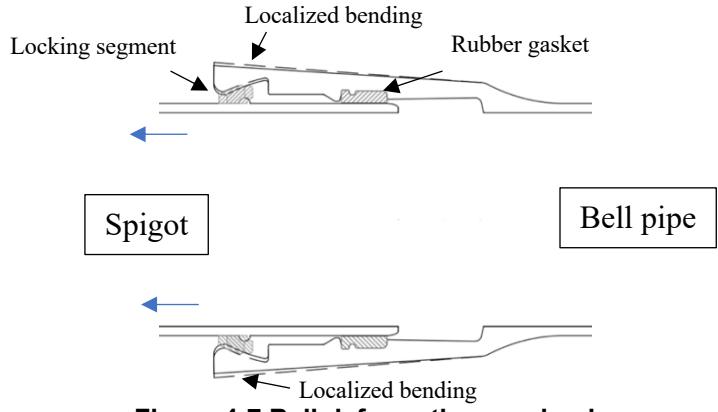


**Figure 4-7 Bell deformation mechanism**

Figure 4-8 presents the axial strain results measured on the spigot. As a unidirectional axial force was applied to the pipe, tensile strains were recorded throughout the spigot sections. The strain magnitudes were similar across all four measured locations (i.e., top, bottom, south, and north), which indicates a uniform distribution of strain and confirms effective force transfer through the locking mechanism.

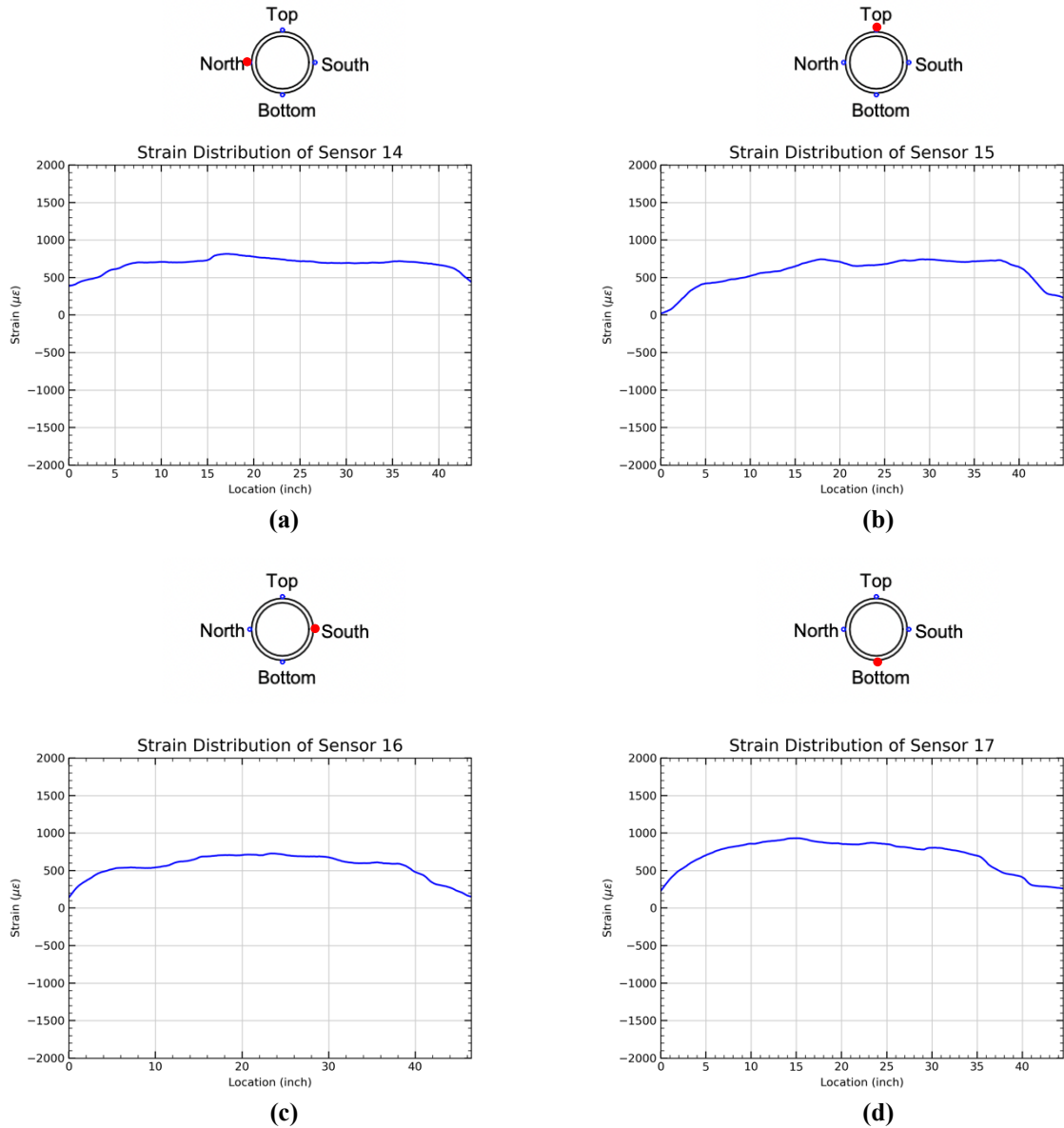


**Figure 4-8 Axial strain development of spigot under 180-kips loading condition. (a) North side, (b) Top side, (c) Bottom side, (d) South side**

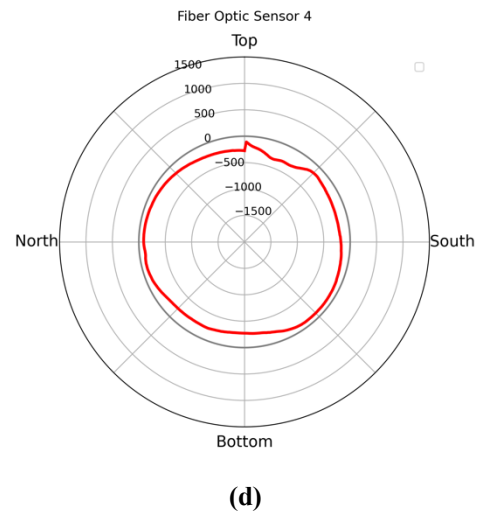
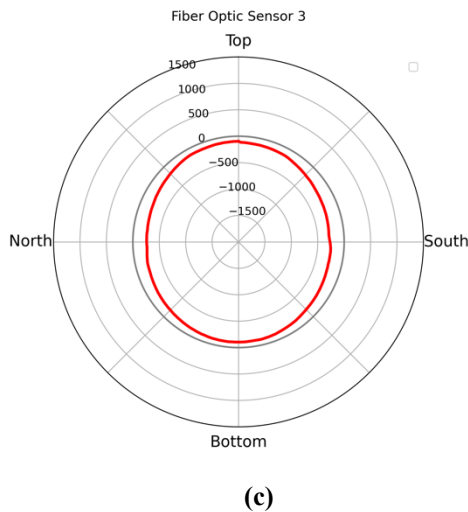
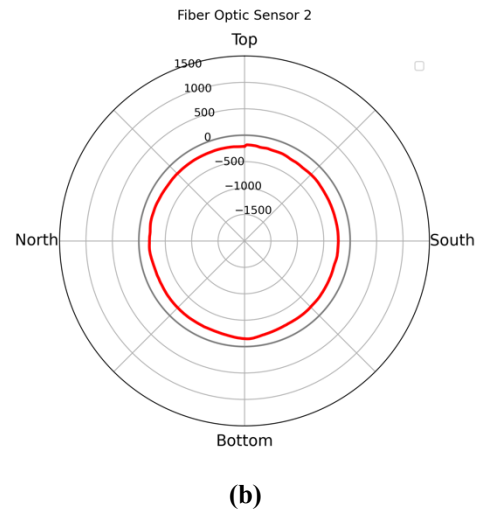
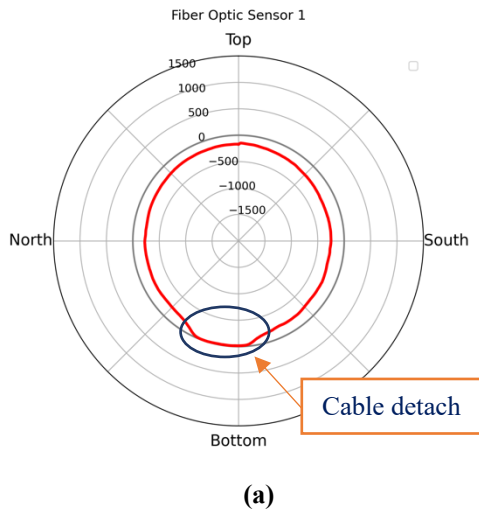
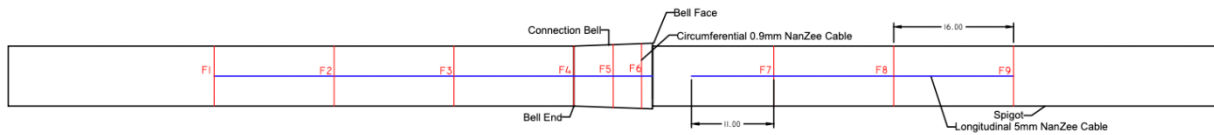
### 4.3 Hoop Strains

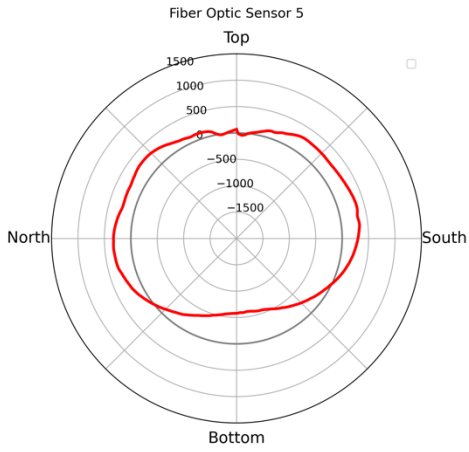
The hoop strain measurements under the 180-kip axial loading condition are plotted in Figure 4-9. Due to Poisson's effect, the circumferential (hoop) strains generally exhibit an opposite trend to the longitudinal strains, but with a smaller magnitude. Since the pipes were primarily under tensile forces in the longitudinal direction, compressive strains were recorded in the hoop direction by the sensors located along the pipe (i.e., F1-F4, F7-F9).

The hoop strain behavior in the bell section (F5 and F6) is more complex. As the spigot was pulled, the locking segments inside the bell came into contact with the snap ring on the spigot. The top side of the bell was sealed with a softer rubber retainer instead of stiffer locking

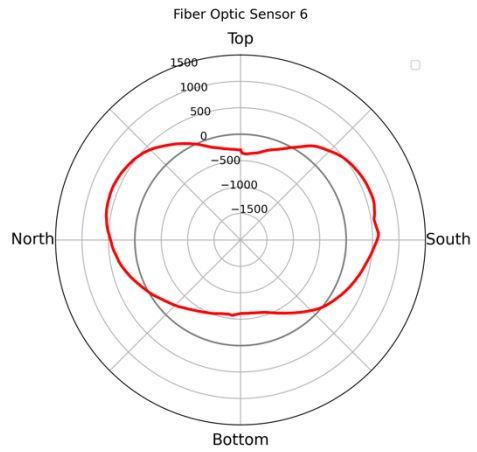
segments, causing compressive strains on the top and bottom sides and tensile strains on the north and south springline sides. The bell squatted in the vertical direction as the locking segments pulled out. Sensor F6, which is closest to the locking segments, clearly reflects this behavior, showing distinct patterns of strain. A similar, yet smaller, pattern is visible on Sensor F5, which is located farther from the locking segments in the middle of the bell section. Similar phenomnom was observed in the previous two tests.

Comparing the strain magnitudes on Sensors F5 and F6 between the top and bottom sides, the compressive strain is noticeably larger on the bottom side than the top. This difference is likely due to the gap on the snap ring on the top side and the presence of the rubber gasket, which replaced the locking segment on the top. Consequently, less force was transferred on the top side, leading to reduced strain in that area.

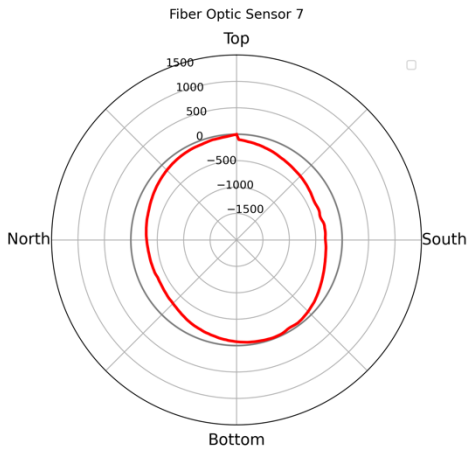




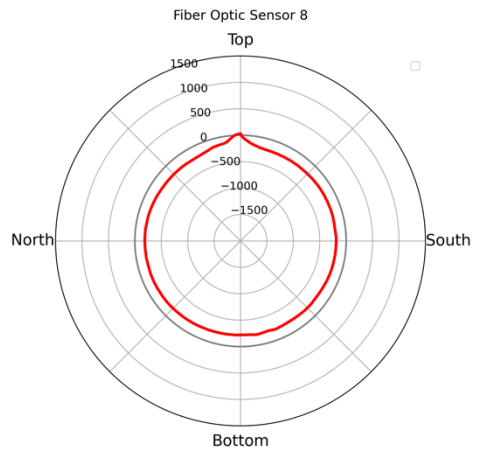
(e)



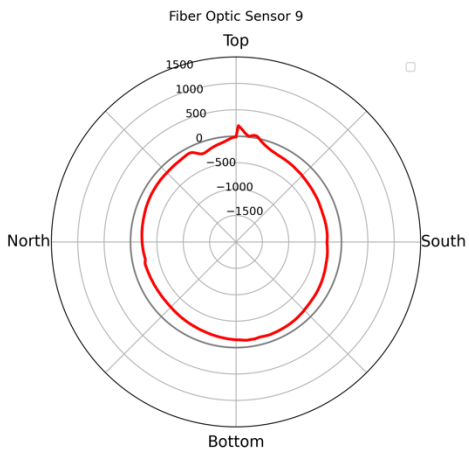
(f)



(g)



(h)



(i)

Figure 4-9 Strain distribution in the circumferential direction under 180-kips loading condition.

Figure 4-10 presents a waterfall plot depicting the strain versus time and location for Sensor F6 (positioned on the bell near the locking segments) and Sensor F7 (located on the spigot closest to the bell face). The plots illustrate the strain evolution over time up to the point of failure. F6 shows squatting behavior of the bell section, whereas F7 shows more compressive force transferred at the springline locations rather than the top and bottom sections.

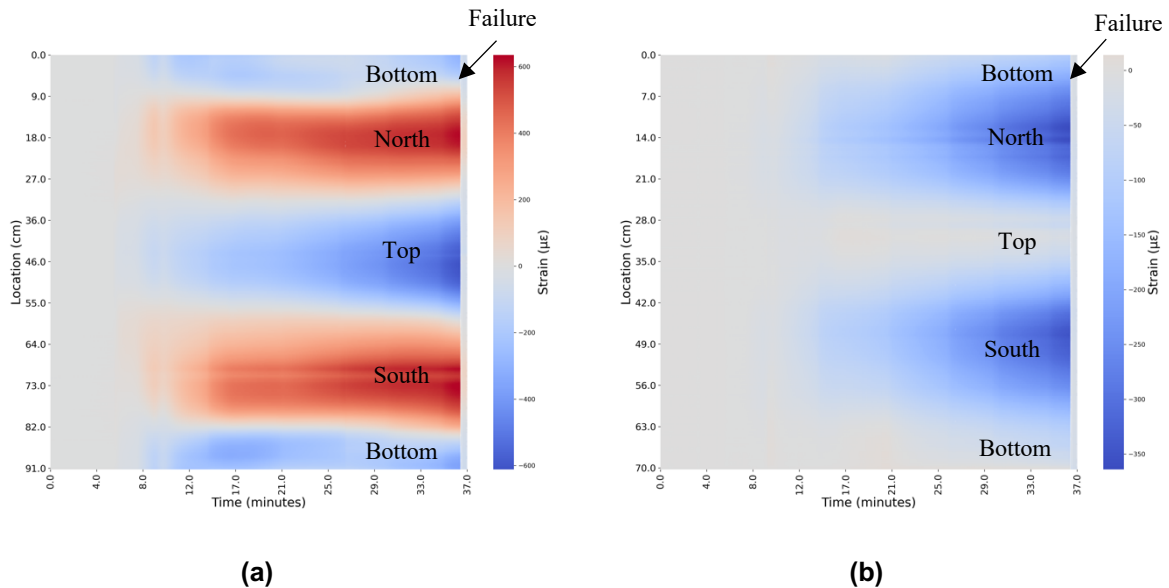


**Figure 4-10 Waterfall plot of sensors on the bell and spigot (a) Sensor 6 (b) Sensor 7**

The better force transfer at the spring line may be attributed to the gap at the top of the snap ring and the rubber positioned within the top of the single slot. Since the snap ring is not fully attached to the spigot, relative movement between the two components might occur. Consequently, as the bell contracts at the top and bottom sides and expands at the spring lines, the spigot could shift upward, potentially widening the gap at the top of the snap ring to accommodate this movement. This upward motion might enhance contact between the spigot and the snap ring along the sides, while reducing contact at the bottom. This mechanism likely results in better force transfer at the spring line and reduced transfer along the vertical axis, as illustrated in Figure 4-11(a). Numerical simulation to investigate this issue will be done as future study.

This phenomenon differs from observations in the previous two tests, where the weld beads were firmly attached to the spigots, preventing relative movement. Additionally, no gap was present at the top of the weld bead. These factors ensured more uniform force transfer, causing the spigot's squatting mechanism to be similar to the bell's squatting behavior, as depicted in Figure 4-11(b).

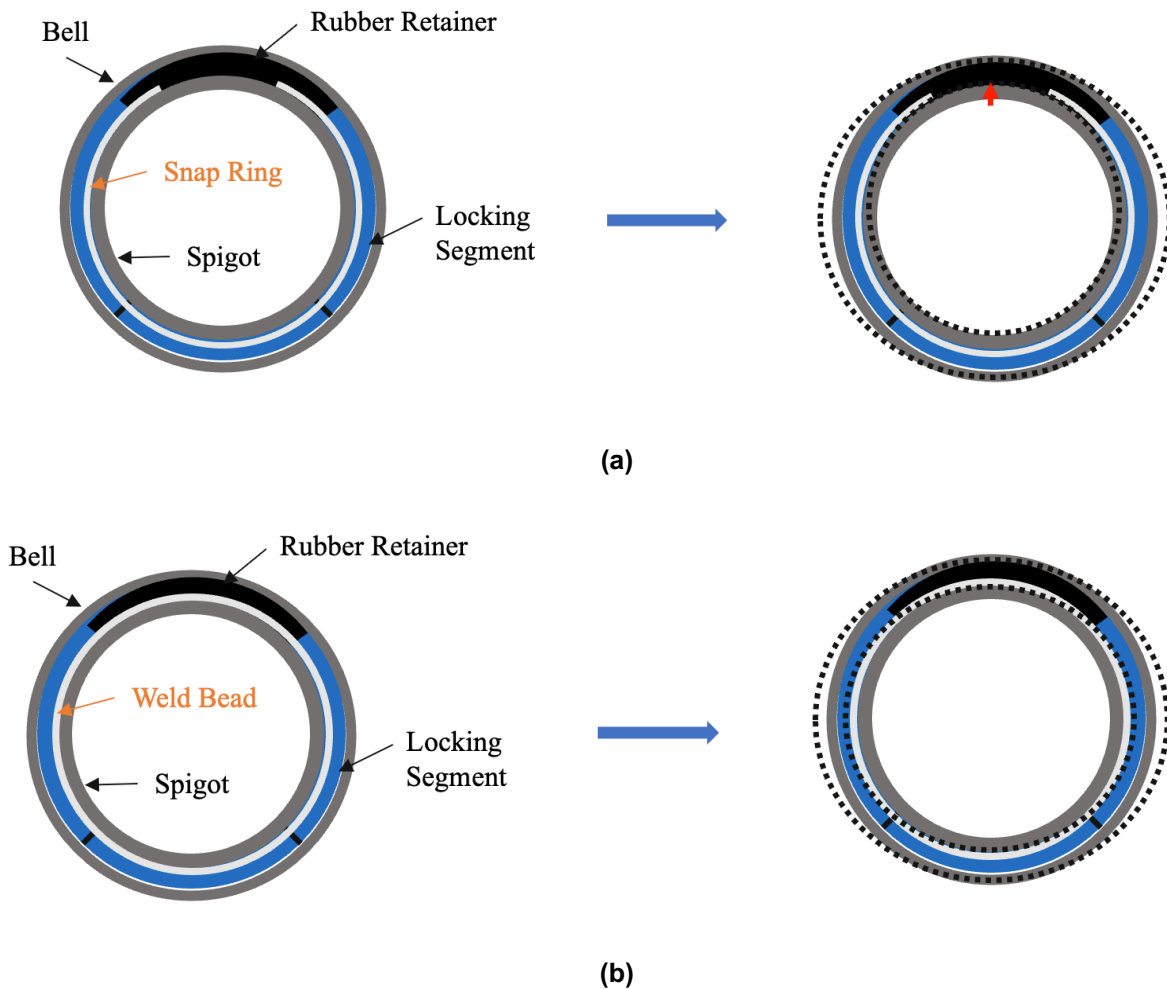


Figure 4-11 Sketch of squatting mechanism (a) Specimen-HDSS (b) Specimen-WB1 & Specimen-WB2

## 5. Conclusion

This report describe results of the tension test conducted on the 8-inch TR-XTREME™ earthquake-resistant ductile iron pipe equipped with HDSS QuikLok on spigot. The results demonstrated that the ultimate axial resistance of the pipe with the HDSS QuikLok locking mechanism is comparable to that of pipes equipped with the factory-manufactured weld bead, with both systems achieving similar maximum axial force capacities. However, differences in failure modes were observed. The spigot failed with the HDSS QuikLok locking case, whereas the bell failed the factory-manufactured weld bead case. This in turn led to difference in axial movement capacity before water leakage occurred.

For the HDSS QuikLok specimen, the spigot failed at a force of 190.3 kips, resulting in immediate water leakage due to the complete detachment of the spigot. In contrast, the previous tests on specimens with weld beads showed that water service could be maintained beyond initial failure, with water leakage occurring only after further axial movement. These differences

are attributed to the distinct failure patterns, particularly the sudden groove failure in the HDSS QuikLok specimen.

The distributed fiber optic sensing (DFOS) data further clarified the strain development in both the longitudinal and circumferential directions, confirming efficient force transfer through the locking mechanism. The strain patterns also revealed the squatting mechanism especially at the bell location to accommodate the locking segments being pulled out. A distinct force transfer mechanism near the bell was observed compared to previous tests. When a weld bead was used, the force transfer was more uniform. However, with a HDSS QuikLok, the force transfer was more concentrated and effective along the spring line.

Overall, while both HDSS QuikLok and the factory weld bead locking mechanisms performed similarly in terms of load-bearing capacity, their differing failure behaviors may influence the decision for field applications where maintaining water service under ground movement conditions is critical.

## 6. Reference

- Chiu, S., Zhang Q., Takhirov S., Soga K. (2023). Direct Tension Testing of 8-in. (200-mm) Diameter TR-XTREME Ductile Iron Pipe. Center for Smart Infrastructure, *University of California, Berkeley*.
- LUNA inc. (2022). ODiSI 6000 Series Optical Distributed Sensor Interrogators. Retrieved from <https://lunainc.com/sites/default/files/assets/files/data-sheet/Luna%20ODiSI%206000%20Data%20Sheet.pdf>
- U.S. Pipe. (2024). TR XTREME Seismic Joint Pipe [Brochure]. [https://www.uspipe.com/wp-content/uploads/USP\\_04\\_TRXTREME\\_SubmittalBook\\_2024\\_digital.pdf](https://www.uspipe.com/wp-content/uploads/USP_04_TRXTREME_SubmittalBook_2024_digital.pdf)
- Wu, J., Jiang, H., Su, J., Shi, B., Jiang, Y., & Gu, K. (2015). Application of distributed fiber optic sensing technique in land subsidence monitoring. *Journal of Civil Structural Health Monitoring*, 5(5), 587-597.

# Appendix A: Distributed Fiber Optic Sensing

Using the physical properties of light, fiber-optic sensing can detect changes in temperature, strain, and other parameters when light travels along a fiber, which uses fiber-optic cables as sensors and can measure over long distances at 100 to 1000s of points on a single cable or multiplexed cables depending on the analyzer used. Compared to the other sensing technologies, fiber-optic sensing has distinct advantages such as small size, light weight, and strong resistance to corrosion and water. Distributed fiber optic sensing consists of two main components, an analyzer, and fiber-optic cables. LUNA ODiSI 6000 series interrogator was used as the analyzer, and NanZee Sensing Technology Co manufactured the fiber-optic cables in the experiments.

## LUNA Interrogator



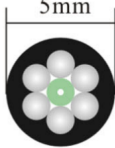
**Figure A-1. LUNA ODiSI 6000 Series optical distributed sensor interrogator (LUNA, 2022)**

LUNA ODiSI 6104 is an optical distributed sensor interrogator that can provide thousands of strain or temperature measurements per meter of a single high-definition fiber sensor. High-Definition H.D.D) Sensors - Strain & Temperature (HD-SC) temperature sensors utilize an advanced interrogation mode of the ODiSI to increase the accuracy of measurements when the sensors are subjected to strain, such as in embedded and surface-mount installations. It can achieve a sensor gauge pitch (the distance between two measurement points) as small as 0.65 mm, a sensor length of up to 50 m, and a measurement rate of up to 250 Hz with an accuracy of less than  $\pm 1$  microstrain.

## Fiber-optic Cable

Two types of fiber optic cables manufactured by NanZee Sensing Technology Co. were used; (a) 5 mm diameter armored cable (NanZee 5mm) and (b) 0.9 mm diameter cable (NanZee 0.9mm). Table 3-2 lists the information on the cables. The difference between the two cables is the thickness and material of the coating. NanZee, a 5mm cable, provides a sheath layer and steel reinforcement, resulting in better protection to the optical core; hence, it can be used for the actual field application. The coating of NanZee 0.9mm cable is thinner than NanZee 5mm cable. NanZee 0.9mm cable has less protection, but a more sensitive strain response is achieved.

**Table A-1 Schematic illustration of the selected strain sensor cable (Wu et al., 2015)**

<b>Brand</b>	NanZee Sensing Technology Co.	NanZee Sensing Technology Co.
<b>Model</b>	Nzs-DSS-C07	Nzs-DSS-C02
<b>Cross section</b>		
<b>Side view</b>		